

Electronic Supplementary Information for

**Remarkably Enhanced Dynamic Oxygen Migration on Graphene Oxide
Supported by Copper Substrate**

Zihan Yan,[†] Wenjie Yang,[†] Hao Yang,[†] Chengao Ji,[†] Shuming Zeng,[†] Xiuyun Zhang,[†] Liang Zhao^{*,†} and Yusong Tu^{*,†}

[†]*College of Physics Science and Technology, Yangzhou University, Jiangsu 225009, China*

^{*}Corresponding Authors: zhaoliang@yzu.edu.cn; ystu@yzu.edu.cn

Contents:

PS. 1: The dynamic oxygen migration pathways for system configurations with top and hcp sites, as well as with bridge site.

PS. 2: The side views of state configurations for oxygen migration on the freestanding GO (fr-GO) and GO@copper.

PS. 3: The energy of various states along the oxygen migration pathways on fr-GO using different exchange functionals including LDA, PBE, PBE-D3, PBE+optB86b-vdW and B3LYP/6-31G(d).

PS. 4: Lists of various distances in R and M on fr-GO and GO@copper.

PS. 5: The analysis of density of states on fr-GO and GO@copper.

PS. 6: The dynamic oxygen migrations for the distribution of the coexistence of the oxidized and unoxidized regions on GO@copper.

PS. 7: The oxygen migration pathways on fr-GO and GO@copper using PBE+optB86b-vdW and PBE-D3 methods.

PS. 8: The tests of effects of vacuum and substrate layers.

PS. 1: The dynamic oxygen migration pathways for system configurations with top and hcp sites, as well as with bridge site.

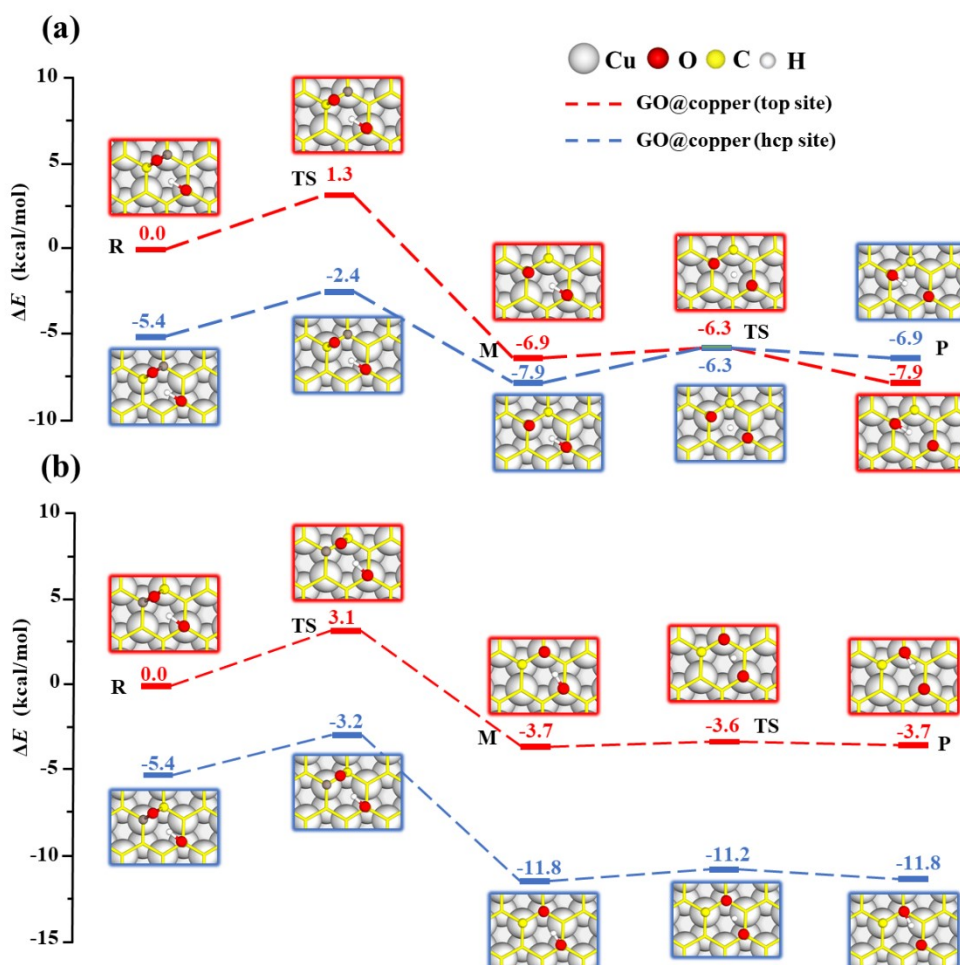


Figure S1. The oxygen migration occurring at the (a) para- and (b) meta-positions of an aromatic ring for the configuration with top and hcp sites on GO@copper using LDA. The hydroxyl-assisted oxygen migration includes the C-O bond breaking reaction and the proton transfer between the dangling oxygen and neighboring hydroxyl for the exchange on the top site (red lines) and the hcp site (blue lines) of GO@copper. Notations: reactants (R), intermediates (M), transition states (TS), and products (P). The energy level of R on GO@copper (top site) is shifted for a better comparison.

Fig. S1 shows the oxygen migrations occurring at the para- and meta-positions of an aromatic ring for the configuration with top and hcp sites on GO@copper. For the oxygen migration occurring at the para-position, the C-O bond breaking and the proton transfer energy barriers are in the range of 0.6-3 kcal/mol. For the new oxygen migration at the meta-position, the barriers of C-O bond breaking and proton transfer reaction are 3.1 kcal/mol and 0.1 kcal/mol for the top site, 2.2 kcal/mol and 0.6 kcal/mol for the hcp site. Compared to the configuration with top and fcc sites (Figs. 2 and 4 in the Communication), the variation of the oxygen migration barriers is negligible.

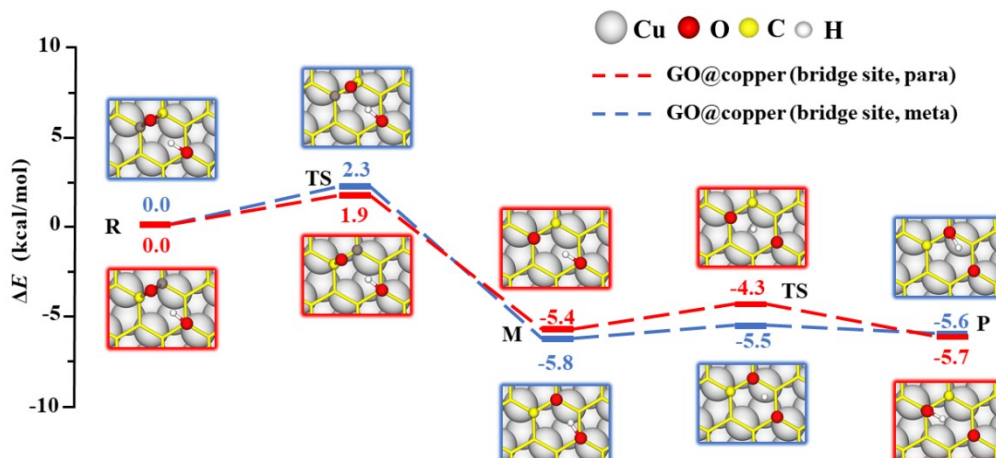


Figure S2. The oxygen migration occurring at the para- (red lines) and meta-positions (blue lines) of an aromatic ring for the configuration via bridge site on GO@copper using LDA. Notations: reactants (R), intermediates (M), transition states (TS), and products (P).

Fig. S2 shows the oxygen migrations occurring at the para- and meta-positions of an aromatic ring for the configuration with bridge sites on GO@copper. The energy barriers of the C-O bond breaking and the proton transfer reactions are in the range of 0.3-2.3 kcal/mol, an indication of the relatively low barriers which are similar to those found for configurations with hcp and fcc sites, or with top and hcp sites. There is another possible configuration of R state in Fig. S2, where the hydroxyl can occupy the adjacent carbon atom. However, this configuration is found to be unstable and the GO will slip. We thus only analyzed the oxygen migration pathways on the current configuration with bridge site.

PS. 2: The side views of state configurations for oxygen migration on the freestanding GO (fr-GO) and GO@copper.

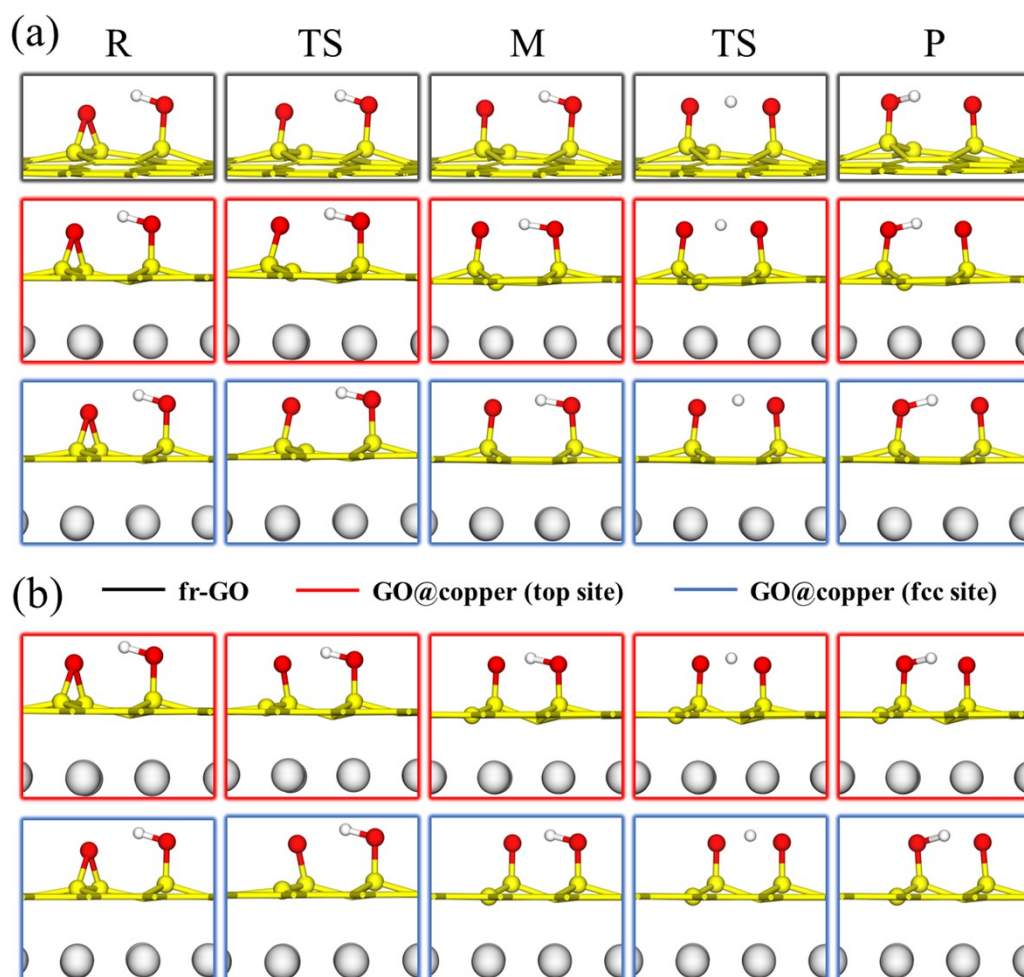


Figure S3. The side views of state configurations for oxygen migration on fr-GO (black boxes) and GO@copper (top sites for red boxes, fcc sites for blue boxes). The side views of the oxygen migrations occur at the (a) para- and (b) meta- positions of an aromatic ring. Notations: reactants (R), intermediates (M), transition states (TS), and products (P).

PS. 3: The calculated energy of various states along the oxygen migration pathways on fr-GO using different exchange functionals including LDA, PBE, PBE-D3, PBE+optB86b-vdW and B3LYP/6-31G(d).

Table S1. The calculated energy of various states along the oxygen migration paths on fr-GO using different exchange functionals including LDA, PBE, PBE-D3, PBE+optB86b-vdW and B3LYP/6-31G(d). Notations: reactants (R), intermediates (M), transition states (TS) and products (P). The energy of R state is shifted to 0 for an easy comparison.

Exchange Functionals	Energy (kcal/mol)				
	R	TS	M	TS	P
LDA	0.0	5.3	3.4	8.0	3.4
PBE	0.0	5.2	1.5	9.6	1.5
PBE-D3	0.0	5.0	1.0	9.3	1.0
PBE+optB86b-vdW	0.0	4.1	0.7	8.1	0.7
B3LYP/6-31G(d)	0.0	3.9	1.2	15.9	1.2

As shown in Tab. S1, the energy barriers of the C-O bond breaking reactions are in the range of 3.9-5.3 kcal/mol and their values are close. While for the proton transfer reaction, LDA gives the lowest barrier (4.6 kcal/mol), PBE-based functionals give moderate values (7.4-8.3 kcal/mol), and B3LYP gives the highest proton transfer energy barrier (14.7 kcal/mol).

PS. 4: Lists of various distances in R and M on fr-GO and GO@copper.

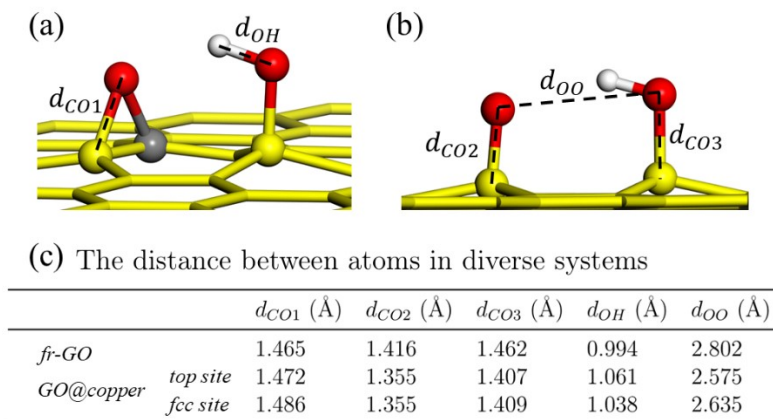


Figure S4. (a, b) Illustrations of distances for C-O bonds (d_{CO1} , d_{CO2} , and d_{CO3}), O-H bond (d_{OH}), and two oxygen atoms (d_{OO}) in reactants (R) and intermediates (M). (c) Lists of various distances in R and M on fr-GO, fcc site, and top site of GO@copper.

Figure S4 compares the variations of bond lengths on GO and GO@copper. Compared to that on GO, the C-O bond of epoxy in R on GO@copper is slightly elongated, indicating that the activity of C-O bond is enhanced. In M, the C-O bonds are significantly shortened, from 1.416 Å to 1.355 Å due to the formation of the dangling C-O bond. The shorter C-O bond in M on GO@copper suggests the stronger strengthen of the C-O bond, explaining the stability of M with the dangling C-O bond. On GO@copper, the O-O distance

in M becomes shorter and the O-H bond is a little elongated, indicating that the proton transfer is more favorable, consistent with the decreased energy barrier of proton transfer on GO@copper.

PS. 5: The analysis of density of states on fr-GO and GO@copper.

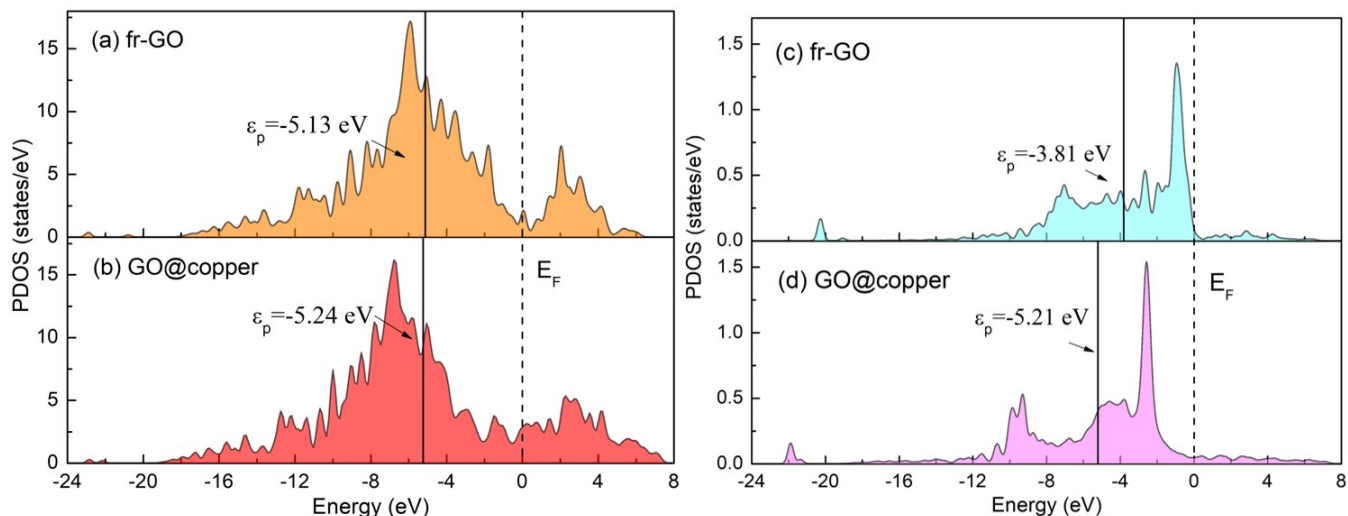


Figure S5. (a, b) Projected density of states (PDOS) of the carbon atoms in R states on fr-GO and GO@copper. (c, d) PDOS of the oxygen atom in the hydroxyl group in M states on fr-GO and GO@copper. The black solid and dotted lines denote the p-band center (ϵ_p) and Fermi level (E_F), respectively.

As shown in Fig. S5, the p-band center (ϵ_p) of carbon atoms of R state on GO@copper (-5.24 eV) is further away from Fermi Level (E_F) than that on fr-GO (-5.13 eV). This indicates a higher level of filling of antibonding states and the weaker C-O bond on GO@copper, explaining that the decreased energy barrier for C-O bond breaking reaction on GO@copper. Similarly, we can see that ϵ_p of oxygen atom in the hydroxyl group of M state on GO@copper (-5.21 eV) is also further away from E_F than that on fr-GO (-3.81 eV), an indication of the weakened O-H bond strength and the decreased proton transfer barrier on GO@copper.

PS. 6: The dynamic oxygen migrations for the distribution of the coexistence of the oxidized and unoxidized regions on GO@copper.

Previously, the oxidized groups on GO sheet is usually treated in an isolated manner or considered to behave independently [*Nat. Chem.* 6, 151 (2014); *Nat. Mater.* 11, 544 (2012)]. However, our recent work demonstrated that the distribution of oxygen functional groups on the basal plane of GO is highly correlated [*Angew. Chem.* 126, 103548 (2014)], which contributes to the description of atomistic structure of GO and is consistent with the previous observations that the coexistence of both unoxidized and oxidized regions. Thus, a pair of hydroxyl and epoxy groups in correlation, rather than a single epoxy

group, is considered in the investigation of the behavior of oxygen groups on fr-GO [*Chin. Phys. Lett.* 37, 066803 (2020)].

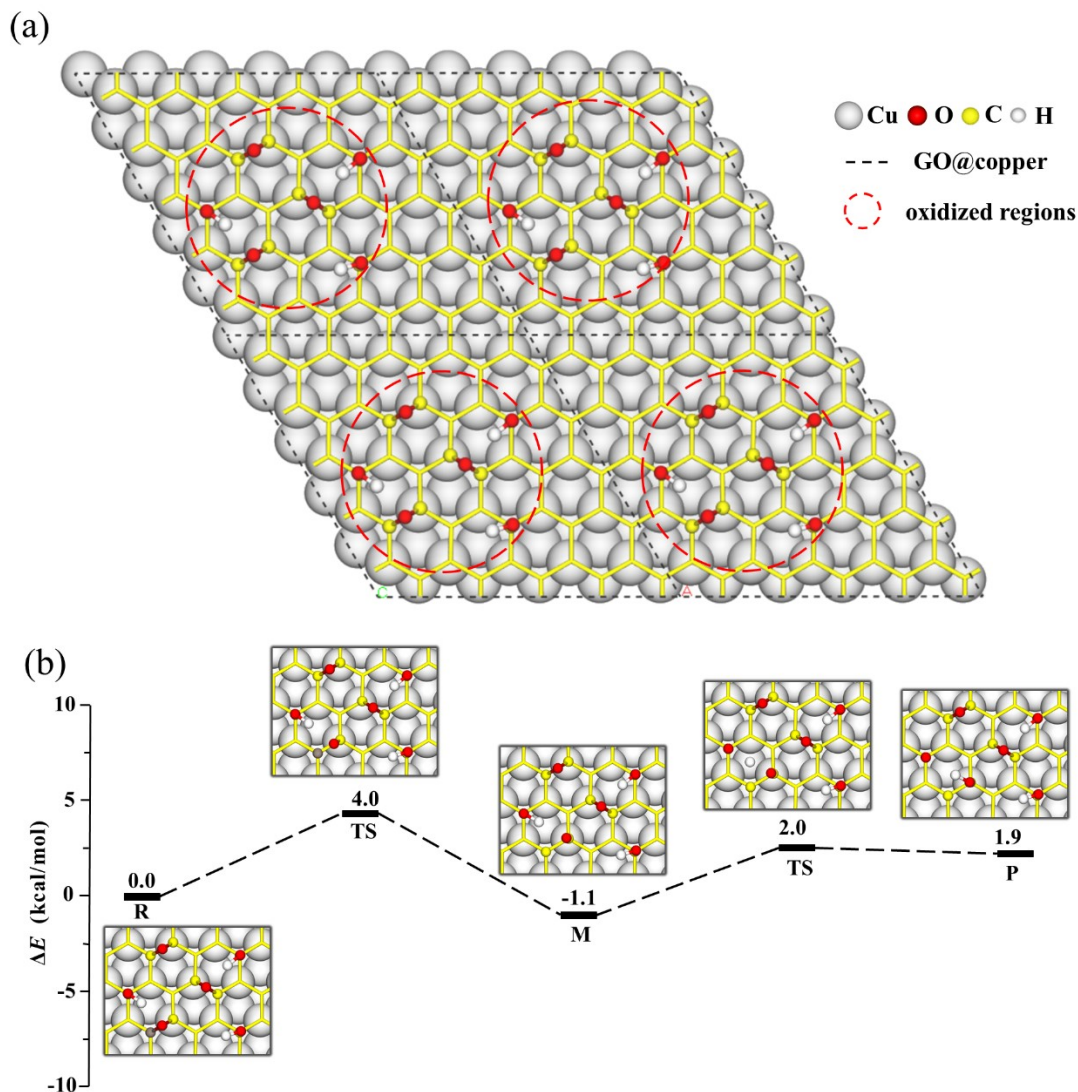


Figure S6. (a) The periodic display of coexistence of oxidized region with the correlated distribution of oxygen groups and unoxidized region on GO@copper. (b) The oxygen migration pathways on GO@copper. Notations: reactants (R), intermediates (M), transition states (TS), and products (P).

For the distribution of the coexistence of oxidized and the unoxidized regions on GO@copper, the energy barriers of oxygen migration are still comparable to thermal fluctuations. As shown in Fig. S6 (b), the epoxy migrates to the para-position occupied by the hydroxyl through C-O bond breaking and proton transfer reactions. The energy barriers for these two reactions are 4.0 and 3.1 kcal/mol, compared to 3.1 and 1.7 kcal/mol for a single pair of hydroxyl and epoxy in the current work (see details in Fig. 2 in the Communication), respectively. The relatively low energy barriers of dynamic oxygen migration are still comparable to thermal fluctuations on GO@copper with the coexistence of oxidized region with the correlated distribution of oxygen groups and the unoxidized region.

PS. 7: The calculated oxygen migration pathways on fr-GO and GO@copper using PBE+optB86b-vdW and PBE-D3 methods.

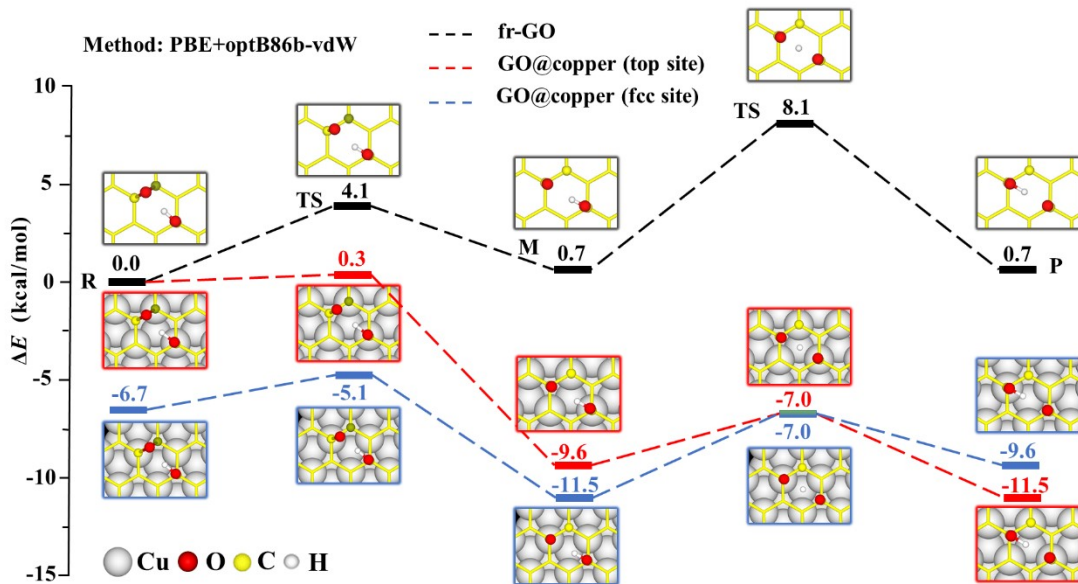


Figure S7. The oxygen migration paths on fr-GO and GO@copper using PBE+optB86b-vdW method. The hydroxyl-assisted oxygen migration includes the C-O bond breaking reaction and the proton transfer between the dangling oxygen and neighboring hydroxyl for the exchange on fr-GO (black lines), on top site (red lines) and fcc site (blue lines) of GO@copper. Notations: reactants (R), intermediates (M), transition states (TS), and products (P). The energy levels of R on fr-GO and GO@copper are shifted to 0 for a better comparison.

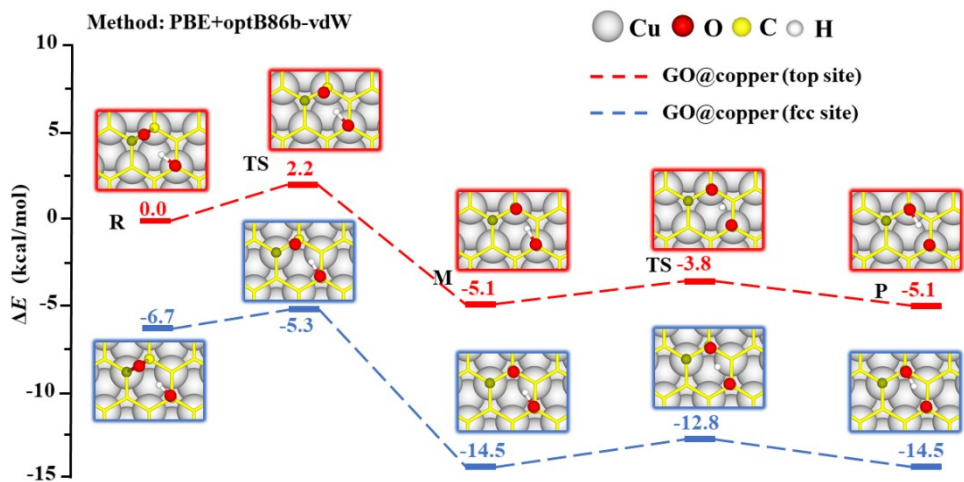


Figure S8. Copper-substrate-induced new reaction pathways of oxygen migration on fr-GO and GO@copper using PBE+optB86b-vdW method. Notations are the same as those in Fig. S7.

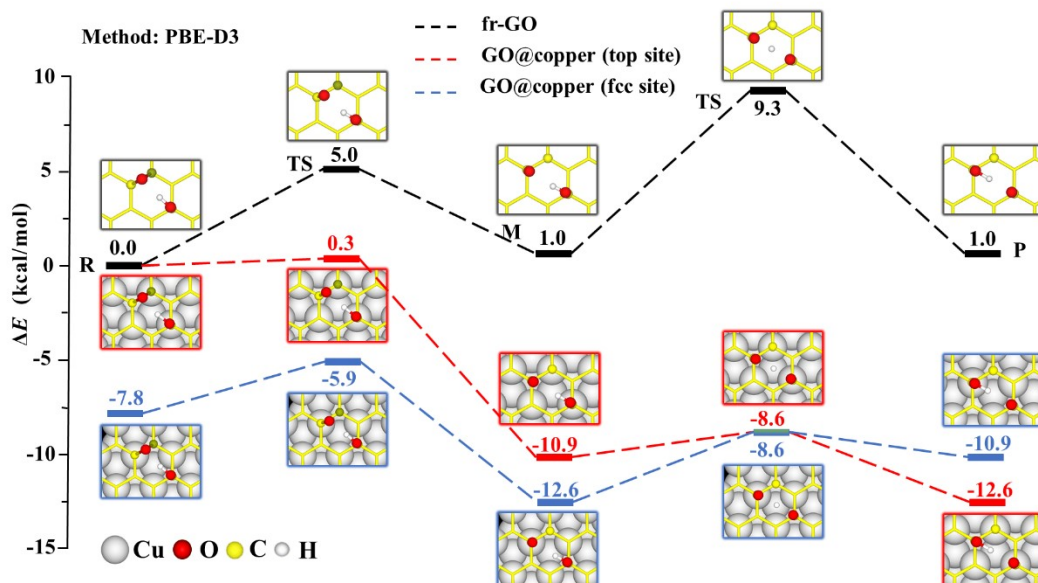


Figure S9. The oxygen migration paths on fr-GO and GO@copper using PBE-D3 method. Notations are the same as those in Fig. S7.

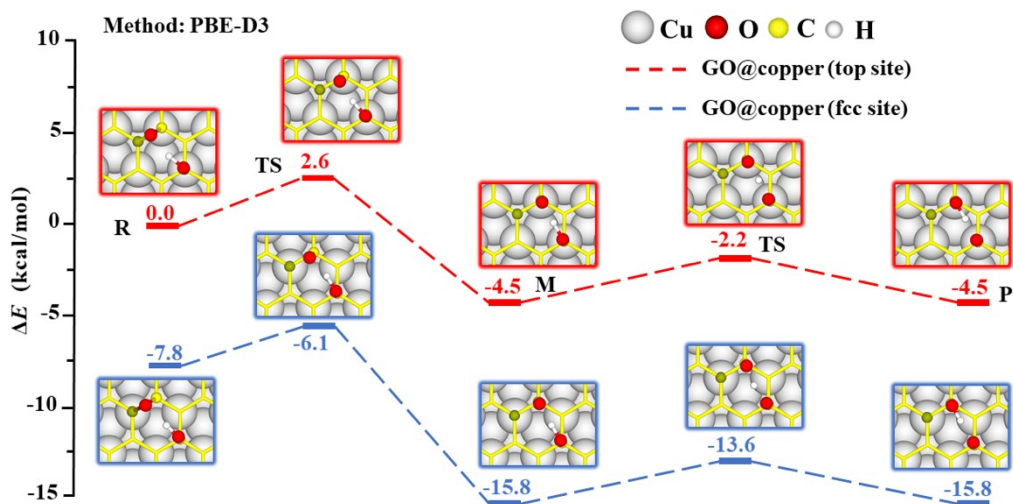


Figure S10. Copper-substrate-induced new reaction pathways of oxygen migration on fr-GO and GO@copper using PBE-D3 method. Notations are the same as those in Fig. S7.

We have supplemented extra DFT calculations using PBE functional with the vdW correction: PBE+optB86b-vdW (Figs. S7 and S8) and PBE-D3 (Figs. S9 and S10). As shown in Fig. S7, for fr-GO, the C-O bond breaking reaction has an energy barrier of 4.1 kcal/mol whereas there is a relatively high

barrier of 7.4 kcal/mol for the proton transfer. However, for the top site of GO@copper, the energy barrier for the C-O bond breaking reaction reduces to 0.3 kcal/mol, and the energy barrier for the proton transfer reduces to 2.6 kcal/mol. The decrease of energy barriers for the C-O bond and proton transfer reactions can be also found for the fcc site, where the barriers are 1.6 kcal/mol and 4.5 kcal/mol, respectively. Moreover, for the new oxygen migration occurring at the meta-position of an aromatic ring on GO@copper, the reaction barriers are all in the range of 1.3-2.2 kcal/mol, as shown in Fig. S8. The results using PBE-D3 method in Figs. S9 and S10 also show the decrease of energy barriers as that using PBE+optB86-vdW. These decreased barriers for the top and fcc sites on GO@copper compared to those for fr-GO, all indicate that the presence of copper substrate can reduce the oxygen migration barriers and further promote the dynamic oxygen migration.

PS. 8: The tests of effects of vacuum and substrate layers.

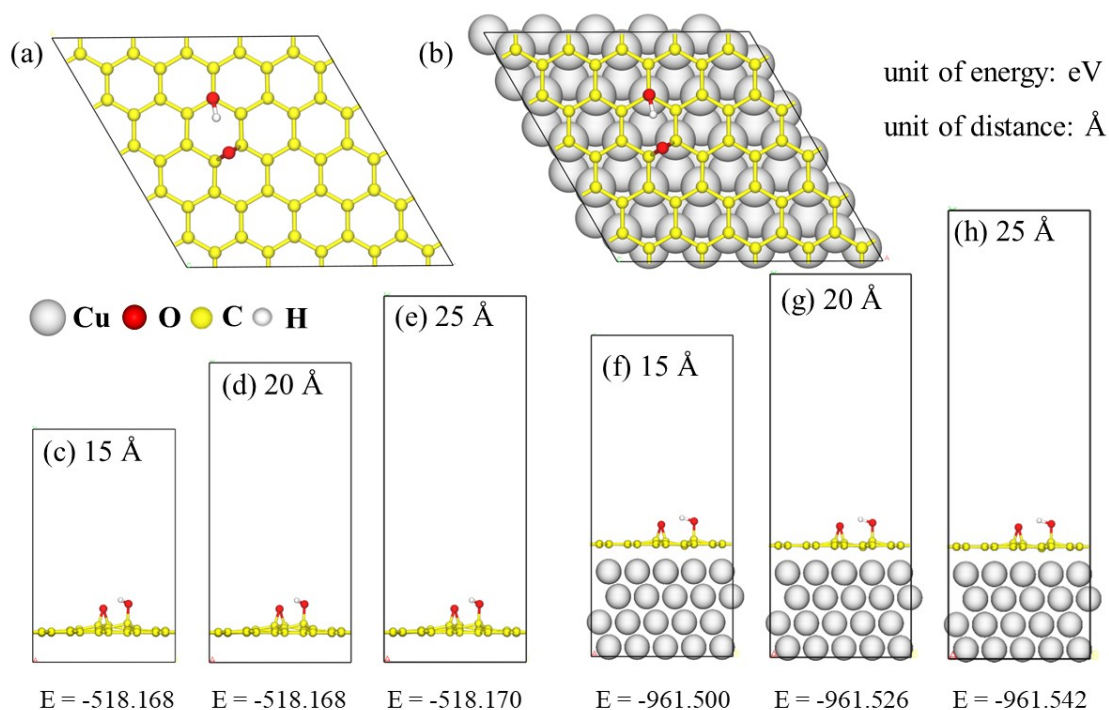


Figure S11. The (a,b) top and (c-h) side views of supercell structures of R states of fr-GO and GO@copper (top site) with different thicknesses of vacuum layers (15, 20, and 25 Å). The system total energy is denoted by E.

The effect of vacuum on the structures of fr-GO and GO@copper has been checked at different thicknesses of vacuum layers (15, 20, and 25 Å). As shown in Fig. S11, the geometry structures of the reactant states of fr-GO and GO@copper (top site) are unchanged. This can also be seen from the negligible variation of the total energy of the system, which is within 1 meV/atom. These results indicate that the vacuum layer of 15 Å in the z-direction is enough for both fr-GO and GO@copper.

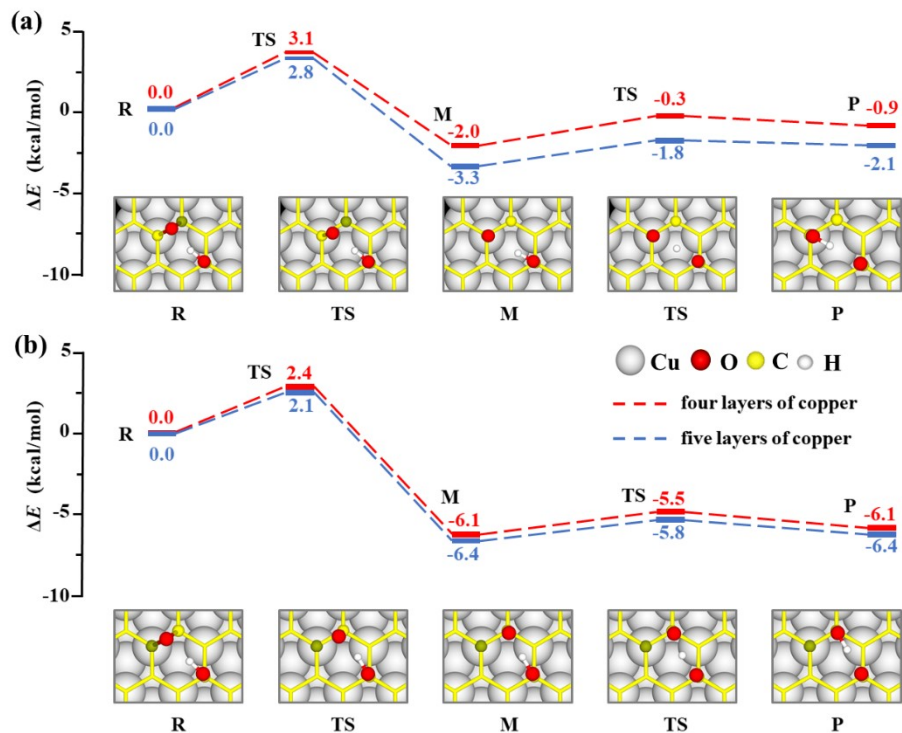


Figure S12. The reaction pathways of oxygen migration occurring at (a) para- and (b) meta-positions of an aromatic ring on GO@copper (fcc site) with four (red lines) and five (blue lines) layers copper atoms. Notations: reactants (R), intermediates (M), transition states (TS), and products (P). The energy level of R on GO@copper (fcc site) is shifted for a better comparison.

We have compared the energy barriers of oxygen migration on the five-layers copper substrate with those on the four-layers copper substrate. From Fig. S12, we can see a small variation of energy barriers of oxygen migration indicating that the thickness of copper substrate has a negligible influence on the energy barrier oxygen migration.